**This document is downloaded from DR-NTU (https://dr.ntu.edu.sg)
Nanyang Technological University, Singapore.**

A nano-opto-mechanical pressure sensor via ring resonator

Zhao, X.; Tsai, J. M.; Cai, H.; Ji, X. M.; Zhou, J.; Bao, M. H.; Huang, Y. P.; Liu, Ai Qun.; Kwong, Dim Lee.

2012

Zhao, X., Tsai, J. M., Cai, H., Ji, X. M., Zhou, J., Bao, M. H., et al. (2012). A nano-opto-mechanical pressure sensor via ring resonator. Optics Express, 20(8), 8535-8542.

https://hdl.handle.net/10356/95386

https://doi.org/10.1364/OE.20.008535

© 2012 Optical Society of America. This paper was published in Optics Express and is made available as an electronic reprint (preprint) with permission of 2012 Optical Society of America. The paper can be found at the following official DOI: [http://dx.doi.org/10.1364/OE.20.008535]. One print or electronic copy may be made for personal use only. Systematic or multiple reproduction, distribution to multiple locations via electronic or other means, duplication of any material in this paper for a fee or for commercial purposes, or modification of the content of the paper is prohibited and is subject to penalties under law.

Downloaded on 25 Aug 2022 23:21:38 SGT

A nano-opto-mechanical pressure sensor via ring resonator

X. Zhao,[1,2,3] J. M. Tsai,[2] H. Cai,[2] X. M. Ji,[1,4] J. Zhou,[1] M. H. Bao,[1] Y. P. Huang,[1] D. L. Kwong,[2] and A. Q. Liu[1,2,3,*]

[1] *ASIC and System State Key Lab, Department of Microelectronics, Fudan University, Shanghai 20043, China*
[2] *Institute of Microelectronics, A*STAR (Agency for Science, Technology and Research), 11 Science Park Road, Science Park II, 117685 Singapore*
[3] *School of Electrical & Electronic Engineering, Nanyang Technological University, 639798 Singapore*
[4] *xmji@fudan.edu.cn*
[*] *eaqliu@ntu.edu.sg*

Abstract: This paper reports a nano-opto-mechanical pressure sensor based on nano-scaled ring resonator. The pressure is measured through the output spectrum shift which is induced via mechanical deformation of the ring resonator. The sensitivity as high as 1.47 pm/kPa has been experimentally achieved which agrees with numerical prediction. Due to the strong variation of sensitivity with different ring radius and thickness of the diaphragm, the pressure sensor can be used to form an array structure to detect the pressure distribution in highly accurate measurement with low-cost advantages. The nano-opto-mechanical pressure sensor has potential applications such as shear stress displacement detection, pressure wave detector and pressure mapping etc.

©2012 Optical Society of America

OCIS codes: (230.4685) Optical microelectromechanical devices; (230.5750) Resonators; (120.5475) Pressure measurement; (080.1238) Array waveguide devices.

References and links

1. Y. C. Chao, W. J. Lai, C. Y. Chen, H. F. Meng, H. W. Zan, and S.-F. Horng, "Low voltage active pressure sensor based on polymer space-change-limited transisitor," Appl. Phys. Lett. **95**(25), 253306 (2009).
2. M. Esashi, H. Komatsu, and T. Matsuo, "Biomedical pressure sensor using buried piezoresistors," Sens. Actuators A Phys. **4**, 537–544 (1983).
3. C. S. Sander, J. W. Knutti, and J. D. Meindl, "A monolithic capacitive pressure sensor with pulse-period output," IEEE Trans. Electron. Dev. **27**(5), 927–930 (1980).
4. D. D. Bruyker and R. Puers, "Thermostatic control for temperature compensation of a silicon pressure sensor," Sens. Actuators A Phys. **82**(1-3), 120–127 (2000).
5. M. C. Oh, J. W. Kim, K. J. Kim, and S. S. Lee, "Optical pressure sensors based on vertical directional coupling with flexible polymer waveguides," IEEE Photon. Technol. Lett. **21**(8), 501–503 (2009).
6. D. Donlagic and E. Cibula, "All-fiber high-sensitivity pressure sensor with SiO_2 diaphragm," Opt. Lett. **30**(16), 2071–2073 (2005).
7. Y. Zhu and A. Wang, "Miniature fiber-optic pressure sensor," IEEE Photon. Technol. Lett. **17**(2), 447–449 (2005).
8. Y. F. Chau, H. H. Yeh, and D. P. Tsai, "Significantly enhanced birefringence of photonic crystal fiber using rotational binary unit cell in fiber cladding," Jpn. J. Appl. Phys. **46**(43), L1048– L1051 (2007).
9. B. J. Luff, J. S. Wilkinson, J. Piehler, U. Hollenbach, J. Ingenhoff, and N. Fabricius, "Integrated optical Mach–Zehnder biosensor," J. Lightwave Technol. **16**(4), 583–592 (1998).
10. M. Ohkawa, M. Izutsu, and T. Sueta, "Integrated optic pressure sensor on silicon substrate," Appl. Opt. **28**(23), 5153–5157 (1989).
11. N. Pelletier, B. Bêche, N. Tahani, J. Zyss, L. Camberlein, and E. Gaviot, "SU-8 waveguiding interferometric micro-sensor for gage pressure measurement," Sens. Actuators A Phys. **135**(1), 179–184 (2007).
12. A. Méndez, "Fiber bragg grating sensors: a market overview," Proc. SPIE **6619**, 661905 (2007).
13. E. Udd and B. W. Spillman, *Fiber Optic Sensors: An Introduction for Engineers and Scientists* (John Wiley & Sons, 2011).
14. W. P. Eaton and J. H. Smith, "Micromachined pressure sensors: review and recent developments," Smart Mater. Struct. **6**(5), 530–539 (1997).

#161085 - $15.00 USD Received 10 Jan 2012; revised 9 Feb 2012; accepted 9 Feb 2012; published 28 Mar 2012

15. C. T. Peng, J. C. Lin, C. T. Lin, and K. N. Chiang, "Performance and package effect of a novel piezoresisitive pressure sensor fabricated by front-side etching technology," Sens. Actuators A Phys. **119**(1), 28–37 (2005).
16. I. Kiyat, C. Kocabas, and A. Aydinli, "Integrated micro ring resonator displacement sensor for scanning probe microscopies," J. Micromech. Microeng. **14**(3), 374–381 (2004).
17. G. N. De Brabender, J. T. Boyd, and G. Beheim, "Integrated optical ring resonator with micromechanical diaphragm for pressure sensing," IEEE Photon. Technol. Lett. **6**(5), 671–673 (1994).
18. M. H. Bao, *Analysis and Design Principles of MEMS Devices* (Elsevier, 2005).
19. S. U. Pillai, *Array Signal Processing* (Springer-Verlag, 1989).
20. H. M. Berger, "A new approach to the analysis of large deflections of plates," J. Appl. Mech. **22**, 465–472 (1955).
21. K. Okamoto, *Fundamentals of Optical Waveguides* (Elsevier, 2006).
22. K. Ohtani and M. Baba, "Shape Recognition for Transparent Objects Using Ultrasonic Sensor Array," SICE, 2007 Annual Conf. 1813–1818 (2007).

1. Introduction

A pressure sensor is a transducer which transforms measured pressure to detectable electrical or optical signals which are often referred as electrical pressure sensor and optical pressure sensor, respectively. Electrical pressure sensors have been intensively studied due to their vast applications in mechanical, electrical and bio-medical engineering [1–3]. However, many effects were also found to be nontrivial to the performance of electrical pressure sensors. It is found that electrical devices and circuits were sensitive to almost everything such as light, temperature, pressure, electromagnetic (EM) field and humidity, etc [4,5]. During the past thirty years, various ideas have been developed based on optical pressure sensors which have apparent merits such as immunity to electromagnetic interference (EMI), lightweight, small device scale, high sensitivity, and ease in signal transmission [6]. Most of the optical pressure sensors are based on either optical fibers [7,8], or Mach-Zehnder interferometer (MZI) [9–11]. However, optical fibers are difficult to be integrated by using standard silicon fabrication [12,13]. MZI as well as other optical waveguide-based pressure sensors suffer from nonlinear output and difficulty in constructing sensors array. In recent research, optical pressure sensors have been miniaturized using microelectromechanical systems (MEMS). Optical MEMS pressure sensors have been fabricated using many different technologies such as piezoelectric quartz crystals, II–VI compound photoconductors and metal diaphragm [14]. Nano-optical-mechanical pressure sensors based on silicon wafer fabrication advance in mass production and low cost [15], which definitely have great advantage in producing micro-scaled or even nano-scale pressure sensors. In this paper, a novel nano-opto-mechanical pressure sensor based on ring resonator structure [16,17] is proposed to provide a reliable optical pressure sensor with high sensitivity, good linearity of the output, CMOS compatibility and ease in integration.

2. Design and theoretical analysis

The nano-opto-mechanical pressure sensor consists of a circular diaphragm, a ring resonator and a bus waveguide which is shown in Fig. 1(a). The ring resonator is located on the center of the circular diaphragm which can be deformed by the pressure applied. The radius of the ring resonator can be changed because of the shear stress displacement in radius direction, as shown in Fig. 2(a) and 2(b). The gap between the bus waveguide and the ring resonator is 200 nm as shown in Fig. 1(b). The broadband signal light is input from one end of the bus waveguide and output from the other. The light is coupled to and resonant within the ring resonator when satisfied the resonance condition. The scattering loss of the ring resonator results in the transmission dips of the output spectra which are dominated by the radius r and effective refractive index n_{eff} of the ring resonator. The ring radius change Δr of the ring resonator induced by the shear stress is the sum of both the deformation of the diaphragm and the displacement of the ring resonator relative to the diaphragm, which are proportional to the cube of the diaphragm and ring resonator thickness, respectively [18]. Hence, the contribution of the displacement of the ring resonator to the change in the ring radius is made negligibly

#161085 - $15.00 USD Received 10 Jan 2012; revised 9 Feb 2012; accepted 9 Feb 2012; published 28 Mar 2012
(C) 2012 OSA

small by designing the diaphragm thickness to be 100 times larger than the height of the ring resonator, so that the radius change of the ring resonator Δr equals to the shear stress displacement on the diaphragm where the ring resonator locates. Therefore, the shear stress induced by the pressure on the diaphragm can be monitored via the spectra shift of the output from the bus waveguide which can be used for the measurement of the pressure. The nano-opto-mechanical pressure sensor array, the integrated optical multiplexer and demultiplexer are shown in Fig. 1(c). The pressure sensor array system can be used to measure the value, phase and direction of the pressure wave because of the difference in the radii of the pressure sensors. The bus waveguide is coupled to a line of rings with different radii which is monitored in real time by the shifting of their resonance frequency at each output port. Therefore, the pressure loaded in each sensor unit can be real-time detected. The phase and the wave front of the pressure wave can be detected by the time difference of the output signal from different sensor units which is detail discussed in [19].

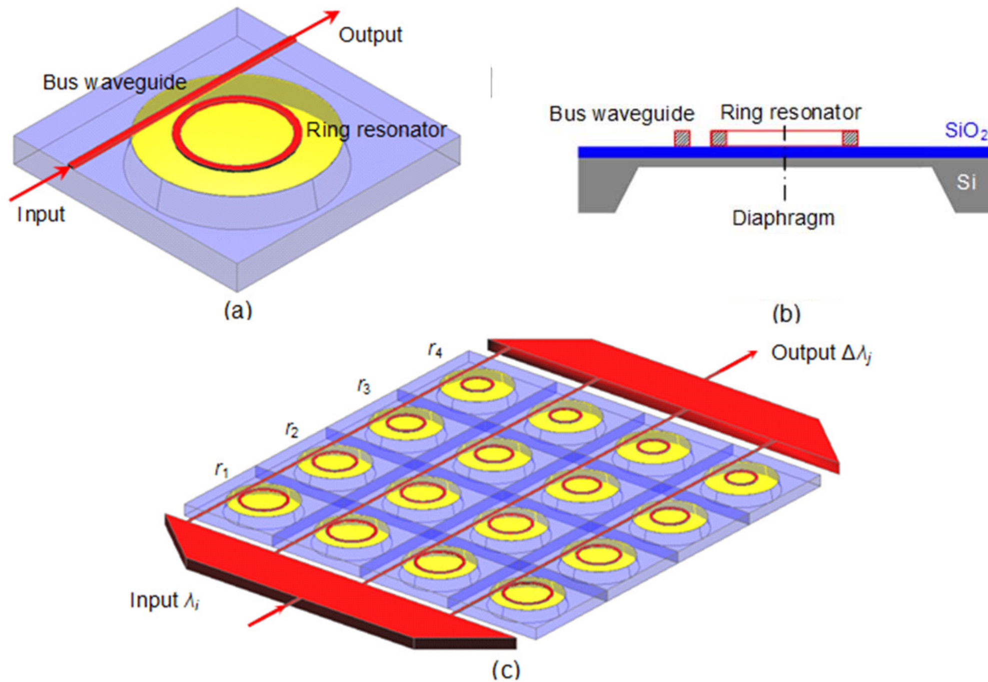

Fig. 1. (a) Schematic of the nano-opto-mechanical pressure sensor. (b) Cross-section of the pressure sensor. (c) The 4 × 4 pressure sensor array.

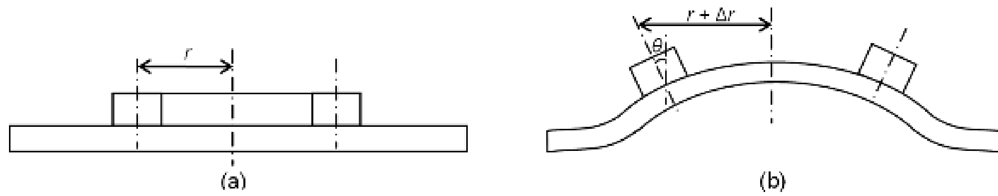

Fig. 2. Schematic illustration of the radius change of the ring resonator Δr due to the shear stress displacement (a) before and (b) after pressure applied on the diaphragm.

2.1 Mechanical design

The radius change of the ring resonator Δr is the function of the applied pressure P on the diaphragm which is dependent on the mechanical properties of the diaphragm. The Δr has

#161085 - $15.00 USD Received 10 Jan 2012; revised 9 Feb 2012; accepted 9 Feb 2012; published 28 Mar 2012
(C) 2012 OSA

rotational symmetry with the z-direction axis at the center of the diaphragm which is circular. Here, a cylindrical coordinate system is setup with the origin at the center of the diaphragm, as shown in Fig. 3(b), where $\Delta r = \Delta r(\rho)$. The u and w refer to the deflections of the diaphragm in ρ-direction and z-direction, respectively. Therefore, the radius change of the ring resonator Δr is equal to the change of deflection of the diaphragm in ρ-direction u which can be expressed as [18,20]

$$\left(\frac{d^2}{dr^2}+\frac{1}{r}\frac{d}{dr}\right)\left(\frac{d^2w}{dr^2}+\frac{1}{r}\frac{dw}{dr}-\gamma^2 w\right)=\frac{P}{D_{eq}} \tag{1a}$$

$$D_{eq}=\frac{1}{3\left(1-v_i^2\right)}\left[\left(h_1-h_0\right)^3+h_0^3+\frac{1}{3}\left(h_2+h_1-h_0\right)^3-\frac{1}{3}\left(h_1-h_0\right)^3\right] \tag{1b}$$

$$\gamma^2=\frac{12}{h^2}\left[\frac{du}{dr}+\frac{u}{r}+\frac{1}{2}\left(\frac{dw}{dr}\right)^2\right] \tag{1c}$$

where γ is the constant of integration, P is the uniform pressure, D_{eq} is the bending rigidity of the equivalent single-layer, v_i, h_i, and E_i are the Poisson's ratio, thickness and Young's modulus of i layer, respectively, i equate 1 or 2 in our design for SiO_2 layer or Si layer, $h_0 = [E_1h_1^2 + E_2h_2(2h_1 + h_2)]/2(E_1h_1 + E_2h_2)$ which is the position of the neutral plane, $h = h_1 + h_2$.

The deflection of the diaphragm in z-direction w is shown in Fig. 3(a) when the pressure P is applied on the diaphragm of 60 kPa. The dashed, solid and dash-dotted lines represent the deflection of the diaphragm in z-direction w with diaphragm thickness h = 15 μm, h = 20 μm and h = 40 μm, respectively. The deflection of the diaphragm in z-direction w reaches the maximum 60.1 nm at origin when r = 0 μm and decrease to zero at the boundary of the diaphragm when the radius of the ring resonator r = 240 μm. However, the deflection in z-direction w is quite different from that of in ρ-direction u which is shown in Fig. 3(b). The deflection of the diaphragm in ρ-direction u reaches the maximum 2.85 nm when $r = r_{max}$ = 137 μm and decreases to zero at the boundary and the center of the diaphragm.

The change of the ring radius Δr as the function of applied pressure P is shown in Fig. 3(c) and Fig. 3(d) at the different diaphragm thickness h and the initial ring radius r, respectively. The change of the ring radius Δr is linearly proportional to the applied pressure when the applied pressure P is ranging from 0 kPa to 60 kPa. Therefore, the change of the ring radius Δr can be expressed as

$$\Delta r = C_1 P \tag{2}$$

where C_1 is the ratio of Δr over P which shows the sensitivity of the ring radius change when the pressure is applied on the diaphragm. C_1 is inversely proportional to the diaphragm thickness which means thinner diaphragm is more sensitive to the pressure applied. Moreover, C_1 reaches the maximum when $r = r_{max}$ = 137 μm for the diaphragm with the radius of 240 μm. Here, C_1 = 0.027 nm/kPa, when h = 20 μm and r = 137 μm as shown in Fig. 3(c) and Fig. 3(d).

#161085 - $15.00 USD Received 10 Jan 2012; revised 9 Feb 2012; accepted 9 Feb 2012; published 28 Mar 2012
(C) 2012 OSA

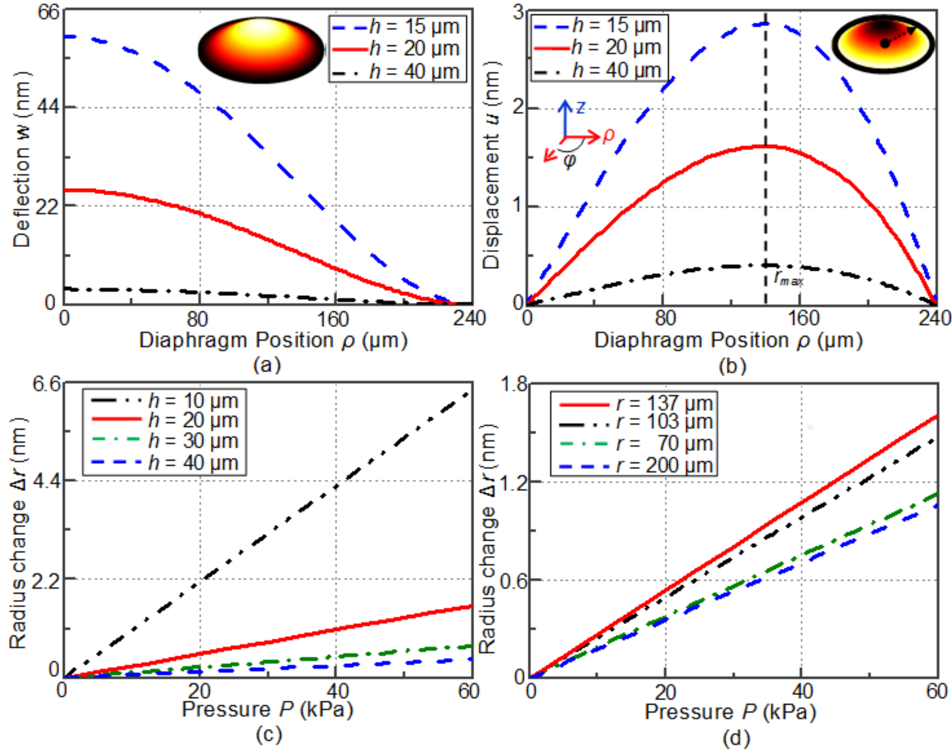

Fig. 3. (a) The deflection of the diaphragm in z-direction as the function of the ρ when the thickness of the diaphragm is 15 μm (dashed line), 20 μm (solid line) and 40 μm (dash-dotted line), respectively. (b) The deflection in ρ-direction at different diaphragm thicknesses when the applied pressure is 60 kPa. (c) The radius change of the ring resonator Δr as the function of the pressure P at different diaphragm thicknesses when the initial radius of the ring resonator r is 137 μm. (d) The radius change of ring resonator Δr as the function of the pressure P at different initial radius r. when the thickness of the diaphragm is 20 μm.

2.2 Optical design

The relation between the output from the bus waveguide and the change of the ring radius Δr is numerically analyzed for the calibration of the nano-opto-mechanical pressure sensor. Here, the pressure applied on the diaphragm is measured via the shift of the resonant wavelength $\Delta\lambda$ of the output spectrum. The sensitivity of the nano-opto-mechanical pressure sensor can be defined as the ratio $\Delta\lambda/P$. Based on the coupling condition of the ring resonator and the bus waveguide, the resonant wavelength λ can be given by [21]

$$\beta L = \frac{2\pi}{\lambda} n_{eff} 2\pi r = 2m\pi \quad (3)$$

where β is the propagation constant, $L = 2\pi r$ is the length of the ring resonator, n_{eff} is the effective refractive index of the ring resonator at the resonant wavelength λ, m is the mode number. The resonant wavelength shift $\Delta\lambda$ as a function of the radius change Δr can be written as

$$\Delta\lambda = \frac{2\pi n_{eff}}{m} \Delta r \quad (4)$$

Here, the transverse electric (TE) and the transverse magnetic (TM) mode is defined as the propagating mode with the electrical field parallel and perpendicular to the diaphragm plane, respectively. Only TE mode polarization exists in the ring resonator and the bus waveguide

#161085 - $15.00 USD Received 10 Jan 2012; revised 9 Feb 2012; accepted 9 Feb 2012; published 28 Mar 2012
(C) 2012 OSA

since the thickness of the waveguide is designed to be smaller than the cutoff width of TM mode. Therefore, n_{eff} refers to the effective refractive index of TE mode only. The variation of n_{eff} caused by the photo-elastic effect is approximately 10^{-7} which has trivial effect, compared with the change of the ring radius, on the resonant wavelength shift $\Delta\lambda$. As a result, the relationship between the resonant wavelength shift $\Delta\lambda$ and pressure P is obtained by

$$\Delta\lambda = \frac{2\pi n_{eff} C_1 P}{m} = C_2 P \tag{5}$$

where $C_2 = \Delta\lambda/P$ is the sensitivity of the nano-opto-mechanical pressure sensor and $m = 256$.

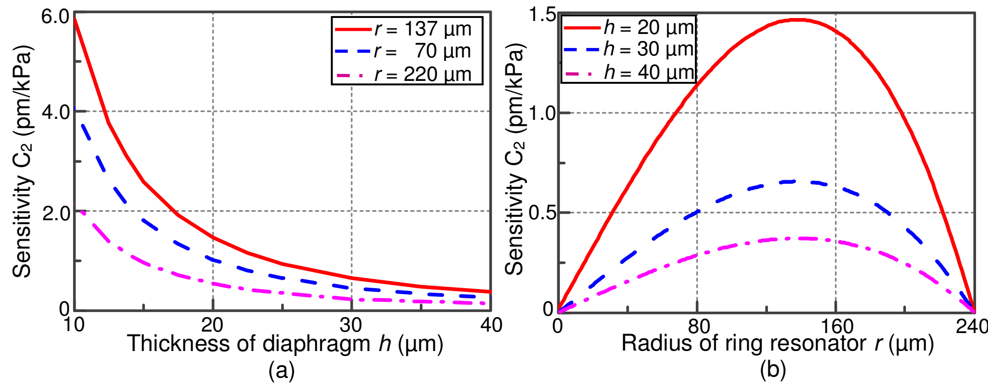

Fig. 4. (a) The sensitivity C_2 versus the thickness of the diaphragm h with different radius of the ring resonator r. (b) The sensitivity C_2 versus the radius of the ring resonator r with different thickness of the diaphragm h.

Figure 4(a) shows the sensitivity C_2 as the function of diaphragm thickness h. The sensitivity C_2 increases exponentially when the diaphragm thickness h is decreasing. When the diaphragm thickness h is 10 µm and the radius of the ring resonator r is 137 µm, the sensitivity C_2 is 5.85 pm/kPa as shown in Fig. 4(a). Here, the diaphragm thickness h is chosen to be 20 µm regarding the fabrication limits. The sensitivity becomes maximum when $r = r_{\max}$ = 137 µm at fixed diaphragm thickness h = 20 µm as shown in Fig. 4(b). Therefore, the radius of the ring resonator is chosen to be 137 µm to achieve the maximum sensitivity.

3. Experimental results and discussions

The SEM images of the fabricated nano-opto-mechanical pressure sensor are shown in Fig. 5. The nano-opto-mechanical ring resonator pressure sensor is fabricated on a standard silicon-on-insulator (SOI) wafer with a silicon structure layer of 220 nm by using nano-photonic silicon fabrication processes. The thickness of silicon dioxide (SiO_2) layer and back side substrate are 2 µm and 720 µm, respectively. The bus waveguide and the ring resonator are patterned by the silicon structure layer using Reactive Ion Etching. Potassium hydroxide (KOH) wet etching is used to the backside etching of the diaphragm with thickness of 20 µm. For comparison, two different sets of parameters are used for the fabrication of the nano-opto-mechanical pressure sensors which are the radii of the ring resonator (r = 70 µm and 137 µm) and the thickness of the diaphragm (h = 20 µm and 40 µm).

Figure 5(a) shows the overview of the pressure sensor with a footprint of 1.8 mm × 1.8 mm which is the same size as the etching window of backside open. Figure 5(b) shows the zoomed-in view of the coupling region between the bus waveguide and the ring resonator. The coupling gap is 200 nm. The bus waveguide and ring resonator have the same rectangular cross-section (450 nm × 220 nm). These nano-scaled structures are used to keep the single-mode propagation of the light.

#161085 - $15.00 USD Received 10 Jan 2012; revised 9 Feb 2012; accepted 9 Feb 2012; published 28 Mar 2012
(C) 2012 OSA

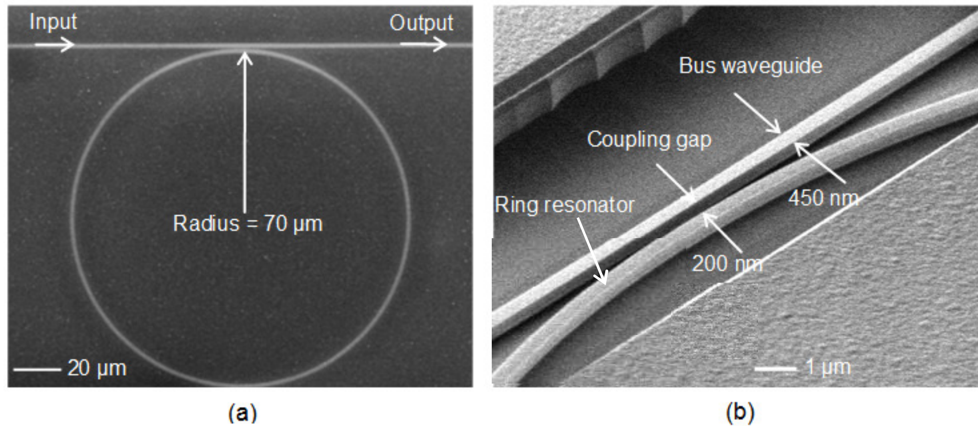

Fig. 5. SEM images of (a) ring resonator with 70-µm radius, and (b) zoom view of the gap between the bus waveguide and ring resonator.

The nano-opto-mechanical pressure sensor is tested by using the fiber-to-chip alignment system (PS-1000, SURUGA SEIKI). The incident broadband source (Amplified Spontaneous Emission) has 8-mW output power over the spectrum ranging from 1570 nm to 1608 nm. The light is input from one end of the bus waveguide and monitored from the other end using an optical spectrum analyzer (AP2052A, Apex Technologies).

The output spectra of the nano-opto-mechanical pressure sensor with different pressures applied to the diaphragm is shown in Fig. 6(a). Here, the diaphragm thickness and the ring resonator radius are 20 µm and 137 µm, respectively. The measured propagation loss of the waveguide is approximately 1.9 dB/cm. The resonance dip wavelength red shifts from 1602.560 nm to 1602.648 nm when the pressure on the diaphragm is increasing from 0 kPa to 60 kPa. The quality factor of the resonance peak is around 9.1×10^3 which is slightly broadened because of the deformation of the ring resonator and the bus waveguide induced by the pressure applied to the diaphragm. The background power loss is increased approximately 2 dB when the pressure is increased from 0 kPa to 60 kPa which is mainly due to the pressure induced bending loss of the bus waveguide. The background power loss does not put a cap on the maximum channel number of multiplexers since the bending of the ring resonators only affects the resonance wavelength. Figure 6(b) shows the resonant wavelength shift $\Delta\lambda$ versus pressure P measured from three different samples. The symbols and the lines represent the measured and simulated results, respectively. The solid, dotted and dashed line show the resonant wavelength shift $\Delta\lambda$ as the function of applied pressure P when r = 137 µm, h = 20 µm; r = 137 µm, h = 40 µm and r = 70 µm, h = 20 µm, respectively which shows a good linearity between the output of the pressure sensor and the measured pressure. The slopes of the lines $C_2 = \Delta\lambda/P$ is equal to the sensitivity of the nano-opto-mechanical pressure sensor. The C_2 is 1.47×10^{-3} nm/kPa, when r is 137 µm, h is 20 µm which is at least 4-fold larger than that of the samples fabricated with the other two sets of parameters. The resolution of the nano-opto-mechanical pressure sensor is 1.36 kPa according to Fig. 6(b). The hysteresis of the nano-opto-mechanical pressure sensor is measured when the pressure is raised up to 60 KPa and then fall back to 0 KPa as shown in Fig. 6(c). The hysteresis uncertainty is measured to be less than 2% when the ring radius r = 137 µm and diaphragm thickness h = 20µm. The output of the pressure sensor is maintained at ± 1% after 4-hour testing which shows the self-induced temperature variation is trivial.

#161085 - $15.00 USD Received 10 Jan 2012; revised 9 Feb 2012; accepted 9 Feb 2012; published 28 Mar 2012
(C) 2012 OSA

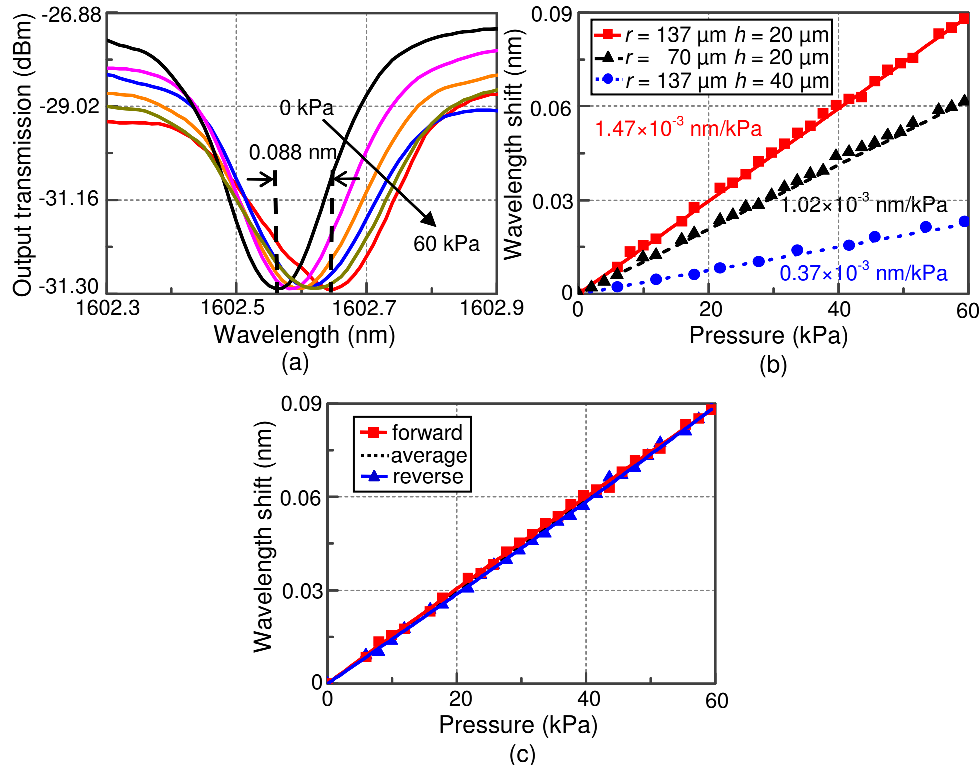

Fig. 6. (a) Transmission spectra at various applied pressures on the diaphragm when the radius of the ring resonator r = 137 μm and the thickness of the diaphragm h = 20 μm. (b) Wavelength shift versus the pressure when r = 137 μm, h = 20μm (solid line), r = 137 μm, h = 40 μm (dotted line) and r = 70 μm, h = 20 μm (dashed line), respectively. (c) Measured hysteresis of wavelength shift versus pressure when r = 137 μm, h = 20μm.

4. Conclusions

In summary, a nano-opto-mechanical pressure sensor based on ring resonator is designed, fabricated and characterized for pressures ranging from 0 kPa to 60 kPa. The sensitivity and resolution of the pressure sensor is 1.47 pm/kPa and 1.36 KPa respectively. The device scale is approximately 1500 μm × 1500 μm and the output signal is linear to the loaded pressure. As the strong variation of detecting frequencies with different ring radius, the pressure sensor array structure can detect the pressure waves and phase through integrated photonic circuit, which can be applied in portable acoustic targeting system and ultrasound shape detection system [22].

This work was supported by the Agency of Science, Technology and Research (A*STAR) with TSRP project (Grant No. SERC 102 165 0084).

#161085 - $15.00 USD Received 10 Jan 2012; revised 9 Feb 2012; accepted 9 Feb 2012; published 28 Mar 2012
(C) 2012 OSA